

Instability-induced localization of matter waves in moving optical lattices

Beata J. Dąbrowska, Elena A. Ostrovskaya, and Yuri S. Kivshar

Nonlinear Physics Centre and ARC Centre of Excellence for Quantum-Atom Optics, Research School of Physical Sciences and Engineering, Australian National University, Canberra ACT 0200, Australia

(Received 6 December 2005; published 7 March 2006)

By using a one-dimensional nonpolynomial nonlinear mean-field model, we numerically analyze the process of the loading of the Bose-Einstein condensate into a moving one-dimensional optical lattice. We demonstrate that the recently observed dynamical instability of the Bloch states of a repulsive condensate in a moving optical lattice can lead to formation of trains of spatially localized wave packets that can be associated with matter-wave gap solitons. We study the characteristic features of this matter-wave localization under realistic conditions by modeling the dynamics of the condensate beyond the onset of dynamical instability.

DOI: [10.1103/PhysRevA.73.033603](https://doi.org/10.1103/PhysRevA.73.033603)

PACS number(s): 03.75.Lm

I. INTRODUCTION

In recent experiments [1,2] the *dynamical instability* of Bose-Einstein condensates (BECs) loaded into a moving one-dimensional optical lattice was observed. This instability arises due to the inherent (repulsive) nonlinearity of matter waves, and it is most profound at the edges of the Bloch wave spectral bands induced by the lattice periodicity. Experimentally observed manifestation of this instability are condensate fragmentation and anomalous heating. However, it is also known that, in the absence of a lattice, such a dynamical (also called *modulational*) instability can trigger another fundamental effect—spatial localization of an attractive condensate in the form of soliton trains [3], similar to the localization observed in the ^7Li BEC [4,5].

Earlier theoretical studies of the Bloch-state stability of a repulsive BEC at the edges of the Brillouin zone (BZ) have also predicted that some of the Bloch states may become modulationally unstable, and that the instability can initiate the formation of spatially localized structures [6]. It can be suggested that such structures represent trains of matter-wave gap solitons [7,8] supported by the combined action of the repulsive nonlinearity and anomalous diffraction at the BZ edges [6,9]. However, localized structures formed as a result of dynamical instability of a repulsive BEC in an optical lattice have not yet been observed.

The purpose of our study is to show that the observation of trains of the spatially localized wave packets triggered by the condensate instability is feasible under realistic conditions of preparation of a condensate at the edge of a Brillouin zone. To this end, we simulate the *loading* of the condensate into a one-dimensional optical lattice from a harmonic trapping potential. We pay particular attention to the process of transition of the condensate to the band edge in the moving lattice and study its subsequent dynamics. To simulate the development of the nonlinearity-induced instability, we employ a one-dimensional nonpolynomial mean-field model that enables the dimensionality reduction in an anisotropic trapping geometry and accounts for the excitations of the condensate in the directions transverse to the lattice.

The paper is organized as follows. First, in Sec. II we describe the mean-field model and then demonstrate in Sec. III that the modulational instability of a nonlinear *homoge-*

neous Bloch state in a lattice does indeed lead to the formation of a train of localized solitonlike states. Next, in Sec. IV we examine a more realistic process of loading the BEC into the optical lattice from a harmonic trapping potential, with subsequent acceleration to the band edge. We show that the resulting *inhomogeneous Bloch state* will also exhibit dynamical instability and form trains of the localized wave packets. Finally, in Sec. V we test the robustness of the spatial localization process in the presence of loss of atoms from the condensate.

II. MODEL

We model the mean-field dynamics of an anisotropic BEC cloud by the time-dependent three-dimensional (3D) Gross-Pitaevskii (GP) equation for the condensate wave function $\Phi(\mathbf{r}, t)$. We assume that the condensate is confined by a strongly anisotropic trapping potential with a tight confinement in the radial (x, y) directions and either a weak harmonic trap or a periodic one-dimensional (1D) optical lattice in z direction. This strong anisotropy of the trapping potential allows for the dimensionality reduction that takes into account the directions transverse to the lattice through a Gaussian ansatz for the radial shape of the wave function, with a z - and t -dependent width [10]. In this approach, the solution to the 3D GP equation $\Phi(\mathbf{r}, t)$ is presented in the form: $\Phi(\mathbf{r}, t) \equiv \Phi(r, z, t) = \chi_{\perp}(r, \sigma) \Psi(z, t)$, where $r \equiv (x, y)$, and

$$\chi_{\perp}(r, \sigma) = \frac{1}{\pi^{1/2} \sigma} \exp(-r^2/2\sigma^2)$$

is *normalized* to unity. The width of the radial wave function, $\sigma^2 = \sqrt{1 + \gamma} |\Psi|^2$, depends implicitly on z and t because of its dependence on $|\Psi|^2$. The wave function $\Psi(z, t)$ obeys the effective 1D nonpolynomial Schrödinger equation (NPSE) [10]

$$i \frac{\partial \Psi}{\partial t} = \left\{ -\frac{1}{2} \frac{\partial^2}{\partial z^2} + V(z, t) + F(|\Psi|^2) \right\} \Psi,$$

$$F(|\Psi|^2) = \gamma\sigma^{-2}|\Psi|^2 + \frac{1}{2}(\sigma^2 + \sigma^{-2}), \quad (1)$$

where $\gamma = g_{3D}/2\pi$, and g_{3D} characterizes atomic interaction due to the two-body scattering. The total number of atoms in the condensate is given by $N = \int dz |\Psi|^2$. If one wants to compare the 3D density with the condensate density obtained from the nonpolynomial model, for example on the symmetry axis of the trap ($r=0$), one needs to take into account that

$$|\Phi(0, z, t)|^2 = |\chi_{\perp}(0, \sigma)|^2 |\Psi|^2 = |\Psi|^2 / \pi \sigma^2.$$

In the model (1) length is measured in units of the oscillator length in the radial dimension $a_{\perp} = (\hbar/m\omega_{\perp})^{1/2}$, time in units of the inverse radial trapping frequency ω_{\perp}^{-1} , and energy in units of $\hbar\omega_{\perp}$. For ^{87}Rb atoms with the mass $m = 1.44 \times 10^{-25}$ kg and the scattering length $a_s = 5.3$ nm confined in a trap with the radial frequency $\omega_{\perp} = 2\pi \times 10^2$ Hz, our length scale becomes $a_{\perp} = 1.08 \mu\text{m}$, and the dimensionless interaction strength is $g_{3D} = 4\pi a_s / a_{\perp} = 6.2 \times 10^{-2}$.

The confining potential of the stationary optical lattice in our model is defined as $V(z, t=0) = V_0 \sin^2(\pi z/d)$, where V_0 is the depth and d is the lattice period. In what follows we set $\pi/d = 1$, which corresponds to the lattice spacing $d = 3.4 \mu\text{m}$. The lattice spacing is proportional to the laser wavelength, $d = \lambda/2 \sin(\theta/2)$, and in the current experiments ranges from approximately 0.4 to 5 μm , depending on the angle θ between the interfering laser beams. The energy scale adopted here is close to the recoil energy of the optical lattice $E_r = \hbar^2 k^2 / 2m$ (where $k = 2\pi/\lambda$); e.g., for the laser wavelength $\lambda = 785$ nm the recoil energy is $E_r = 0.94 \hbar\omega_{\perp}$.

Stationary states of the condensate are described by solutions of Eq. (1) of the form; $\Psi(x, t) = \psi(x) \exp(-i\mu t)$, where μ is the chemical potential. For a noninteracting BEC in a periodic lattice potential, the stationary states are found as $\psi(x) = \phi_k(x) \exp(ikx)$, where the wave vector k belongs to a Brillouin zone of the 1D lattice, and $\phi_k(x) = \phi_k(x+d)$ is a periodic (Bloch) function with the periodicity of the lattice. The spectrum $\mu(k)$ of matter waves in the periodic potential of an optical lattice is characterized by a band gap diagram shown in Fig. 1 (top). Due to its periodicity in k , the spectrum can be reduced to the first Brillouin zone, which extends over $-1 \leq k \leq 1$ (in normalized units).

Finally, we note that the nonpolynomial model (1) was previously successfully used to model matter waves in moving 1D optical lattices [11] and was shown to correctly predict the stability domains of the extended (Bloch) BEC states [12].

III. INSTABILITY OF A HOMOGENEOUS BLOCH STATE

In the presence of the nonlinearity the condensate prepared at the edge of the Brillouin zone suffers from dynamical instability, as demonstrated in recent experiments [1,2]. Theoretically, it has been shown [6], within the framework of the standard 1D GP model, that a Bloch wave at the edge of the BZ [point (b) in Fig. 1] is dynamically unstable while the Bloch wave corresponding to the bottom of the BZ [point (a) in Fig. 1] is stable.

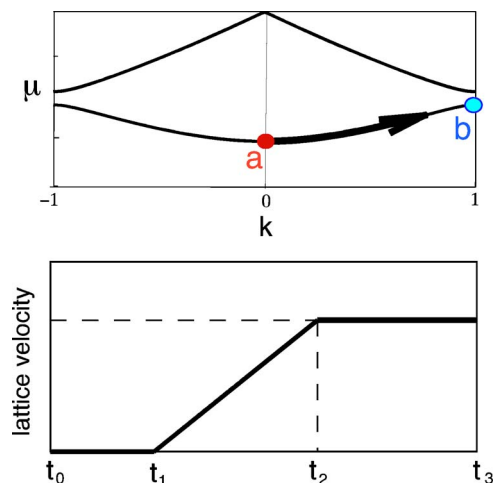


FIG. 1. (Color online) Schematics of the location (in momentum space) of the condensate wave packet relative to the lattice band-gap structure. Points (a) and (b) correspond to the modulationally stable and unstable Bloch states, respectively. Below: schematic time diagram of the adiabatic loading and acceleration of the condensate.

Using the nonpolynomial Schrödinger model (1), we first consider the condensate in the ideal (homogeneous) nonlinear Bloch state prepared at the edge of the Bloch band represented by the point (b) in Fig. 1 (top). In our numerical simulations the development of the dynamical instability of the homogeneous Bloch wave was triggered either by numerical noise or by the weak periodic modulation of an initial state with the period greater than the period of the lattice and the amplitude less than 1% of the Bloch wave amplitude. An amplitude modulated initial Bloch state with the period of the lattice potential, containing $N \approx 5 \times 10^2$ atoms, is shown in Fig. 2(b).

In order to avoid excitations from the edges of the computational domain, absorbing boundary conditions in the form of the Perfectly Matched Layers (PMLs) [13] have been assumed at the edges of the numerical grid. The model Eq. (1) with the PMLs was discretized via the Crank-Nicholson algorithm [13] and solved numerically with the unconditionally stable finite difference time-domain (FDTD) method. In the calculations 32–64 grid points per one lattice site have been used, which resulted in the grid spacing much smaller than the healing length of a homogeneous condensate. Due to the violent dynamics of the instabilities short time steps $dt = 10^{-4}$ were also necessary. Figure 2(a) shows the development of the dynamical instability from a homogeneous Bloch wave and formation of localized wave packets. The computational domain extends over 500 lattice sites, and only a fraction of the entire spatial extent of the condensate is shown in the Fig. 2. In the case of a nonperturbed homogeneous Bloch wave, the dynamical instability commences at $t = 400$. In the case of the initially modulated Bloch state it begins earlier, at $t \approx 250$. The localized states of the condensate shown in Fig. 2(a) are nonstationary, and display persisting oscillations of amplitude. However, they appear to be dynamically robust. In Fig. 2(c) the final state of the evolution at the time $t = 1200$ and with $N \approx 379$ is presented.

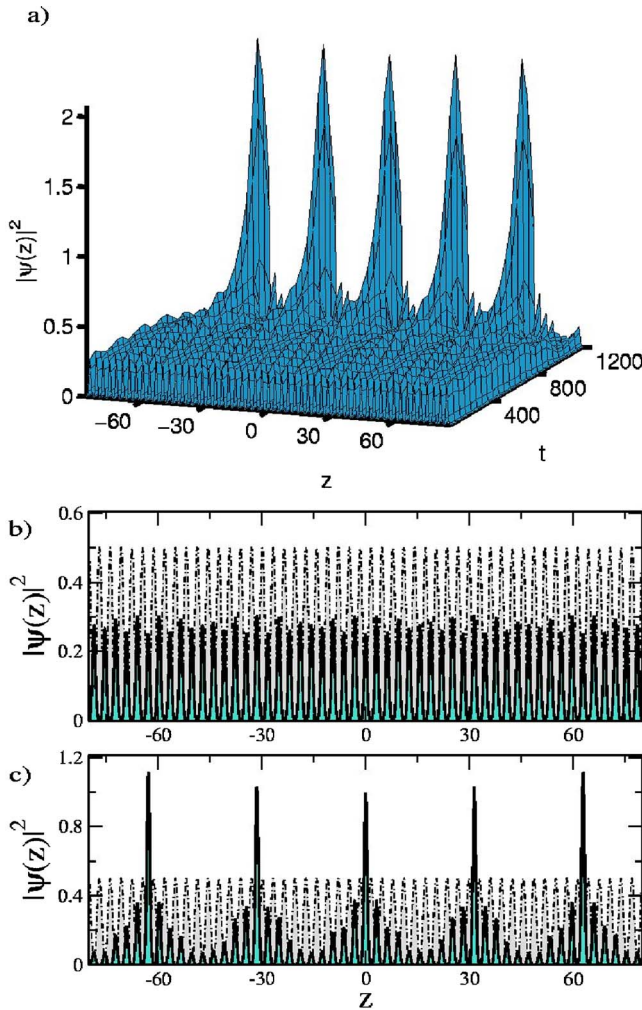


FIG. 2. (Color online) (a) Dynamical formation of localized structures during the evolution of the homogeneous Bloch state shown in (b). (b) Modulationally unstable homogeneous nonlinear Bloch state (solid filled lines) for $\mu=2.49$ and $V_0=5$ found from Eq. (1) and modulated by the function $\sim \cos(z/5)$, plotted together with the lattice potential (dash-dotted filled lines) reduced by the factor of 10. (c) The condensate density profile at $t=1200$ (the maximum density in the localized state is reached at $t \approx 1100$). All parameters are in dimensionless units.

Each localized wave packet has the spatial structure that closely resembles that of a gap soliton from the first spectral gap, found numerically as an exact stationary solution of the model equation (1). The phase structure of the dynamically emerging localized structure is also consistent with the phase structure of a matter-wave gap soliton [7,14].

IV. INSTABILITY OF AN INHOMOGENEOUS BLOCH STATE

The numerical results on the soliton train formation in the nonpolynomial model presented above, as well as those previously obtained for a conventional 1D GP model [6], were produced under the assumption that the initial state of the evolution is an infinitely extended homogeneous Bloch state

at an edge of a Brillouin zone of an infinite lattice potential. In reality, the condensate is loaded into an optical lattice either from a magnetic trap [1] or a crossed optical dipole trap [8], which results in an initial state of a finite extent. A BEC wave packet centered around a particular quasimomentum in a given band is created by either adiabatic loading into a moving optical lattice [1], or ramping up of a static lattice with subsequent linear acceleration to a given velocity [8,15]. In order to investigate the Bloch wave instability in a situation closer to the experimental conditions, we model dynamical formation of an *inhomogeneous* Bloch state from the ground state of a condensate in a 3D harmonic trap by simulating the loading into a stationary optical lattice followed by the acceleration process. Our choice of the loading procedure is motivated by the more relaxed adiabaticity conditions for the case of shallow lattices [16].

We assume the initial harmonic confinement with the aspect ratio $\omega_{\perp}/\omega_z=10^3$ and the chemical potential $\mu=1.1\hbar\omega_{\perp}$, which results in a ground state of $N=6.2 \times 10^3$ atoms with the 3D peak density of $n=3.3 \times 10^{12}$ atoms/cm³. The condensate cloud in the ground state extends over $\sim 10^2$ lattice sites and has a very narrow width of the wave packet in the momentum space that is much smaller than the characteristic energy gap of the Bloch wave spectrum.

To put these numbers into perspective, we note that the experimental observation of the modulational instability [1] required a large ($N \approx 3 \times 10^5$) number of atoms in the condensate and a peak density of around 1.21×10^{14} atoms/cm³. In contrast, the key factor for the experimental observation of a single gap soliton [8] was a low number of atoms in the initial state ($N \approx 900$), and no solitons were observed for the higher ($N \approx 3 \times 10^3$) number of atoms [8]. Our simulations are performed for the number of atoms and condensate density that *far exceed* those required for the formation of a single localized gap soliton, but are sufficient for the observation of the dynamical instability.

The extreme aspect ratio of the trap assumed in our simulations is an order of magnitude larger than that usually achieved with optical trapping [8], and is more readily achievable with BEC in magnetic microtraps [17]; however, the localization effects described below will persist for smaller initial aspect ratios. Moreover, the criterion for the applicability of the 1D mean-field model [18] $N(\omega_z/\omega_{\perp})(a_{\perp}/a_s)^2 \gg 1$ holds for the parameters assumed in our calculations, ensuring that the condensate healing length is much larger than the interparticle distance. The interaction energy of the condensate in our model is comparable to the level spacing of the radial confining potential. This fact justifies the use of the NPSE (1) which takes into account only the lowest radial excitation of the condensate cloud.

The ground state of the condensate in a harmonic trap can be obtained numerically by solving Eq. (1) with the relaxation method [19], and is very well approximated by the Thomas-Fermi solution to the nonpolynomial Schrödinger equation. In our dimensionless units, the Thomas-Fermi profile for a general potential $V(z)$ can be written as follows:

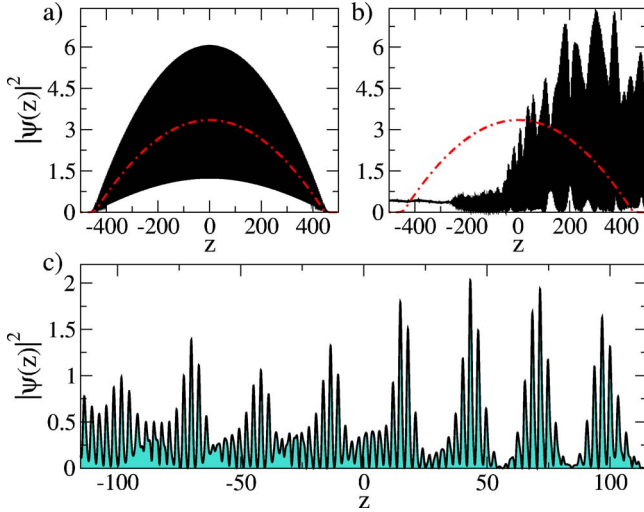


FIG. 3. (Color online) Dynamical formation of localized atomic wave packets during the evolution of a modulationally unstable inhomogeneous Bloch state ($\mu=1.1, V_0=2$). Shown are snapshots of the condensate density profile (a) at the start $V_0=0, v=0$ (dash-dotted line) and at the end $V_0=2, v=0$ (black solid line) of the ramping-up time $t=t_R=200$ and (b) at the end of acceleration time $t=t_R+t_A=500$ ($V_0=2, v=1$). The spatial oscillations in the condensate density cannot be resolved on the scale of the z axis in (a) and (b). (c) Close-up of the central area of the condensate density at $t=600$, i.e., after $t_E=100$ evolution at the band edge ($V_0=2, v=1$). All parameters are in dimensionless units.

$$\psi_{TF}^2 = \frac{2}{9\gamma} \left[(V - \mu)^2 - (V - \mu) \sqrt{(V - \mu)^2 + 3} - 3 \right]. \quad (2)$$

For a harmonic trapping potential, $V = \frac{1}{2} \omega_z^2 z^2$, the Thomas-Fermi radius is $R_{TF} = \omega_z^{-1} \sqrt{2(\mu - 1)}$, which corresponds to $\approx 483 \mu\text{m}$.

The timeline of the procedure of loading the condensate from the harmonic into the periodic confinement is schematically displayed in Fig. 1 (bottom). First, at $t=t_0$ the atomic cloud is suddenly released from the harmonic trap and then the height of the periodic potential of the stationary optical lattice $V_0(t)$ is slowly (and linearly) ramped up over a period $t_R = t_1 - t_0 = 0.32$ s, until it reaches its final value $V_0 = 2\hbar\omega_\perp$. In an experiment, this is achieved by gradual increase of the intensity of the laser beams that produce the standing wave of the optical lattice. During the ramp up, an inhomogeneous Bloch wave corresponding to the bottom edge of the first band, with a period of the lattice potential, forms [see Fig. 3 panel (a)]. The adiabatic ramping up procedure avoids excitations of the second Bloch band [15,16].

The atomic cloud released from the harmonic trap does not spread significantly on the time scale of the ramp up, i.e., while the lattice does not have a significant impact on the condensate dynamics. An estimate of the free expansion time of a matter wave packet corresponding to a ground state of the harmonic oscillator potential with the trapping frequency ω_z shows that the initial width of the wave packet would increase by the factor of two on the time scale $t \approx 5.6$ s, which is much larger than t_R .

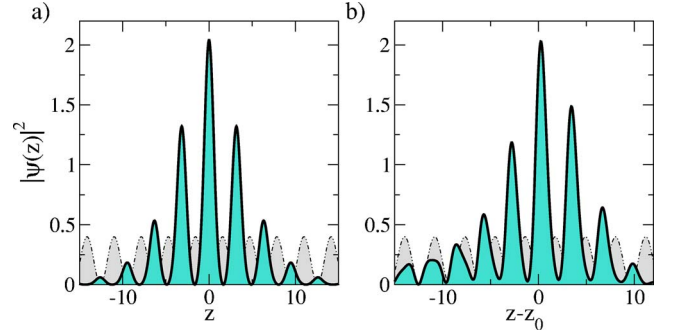


FIG. 4. (Color online) (a) Density profile of a gap soliton of the NPSE for $\mu=1.97$ (solid filled line) and the corresponding lattice potential with $V_0=2$ (dash-dotted filled). The lattice amplitude on the plot is reduced by the factor of 5. (b) Detail of the density of the train shown in Fig. 3(c) in the vicinity of a localized structure centered at $z_0=43$. All parameters are in dimensionless units.

During the second stage, the lattice potential is moved with the constant acceleration (0.14 cm/s^2) over the time $t_A = t_2 - t_1 = 0.48$ s, until the velocity corresponding to the edge of the BZ ($v=1$) is reached. The constant acceleration is achieved experimentally via time-dependent frequency detuning between the two laser beams, and should also be performed adiabatically [16,20] to avoid excitation of the higher bands. As has been previously observed in experimental studies [2], during the acceleration the inhomogeneous Bloch wave exhibits density modulations even before the band edge is reached ($v < 1$). At the edge of the BZ, the amplitude of the modulations becomes comparable with the amplitude of the initial state, as seen in Fig. 3(b). The density of the atomic cloud in Fig. 3 is shown in the frame of the lattice (the lattice potential is moving to the right) with a solid line. The dashed-dotted line is the profile of the initial Thomas-Fermi cloud centered in the moving frame. Faster acceleration results in the cloud lagging behind the lattice without the development of significant density modulations during the time of the acceleration.

Finally, for some time (here $t_E = t_3 - t_2 = 0.16$ s) the condensate is evolved in the potential of the moving lattice. Due to the dynamical instability, the wave packet at the edge of the BZ exhibits violent dynamics. During this evolution the periodic structure of a train of the localized wave packets emerges, see Fig. 3(c). The number of solitonlike structures within a train depends on the density of the initial state, with smaller densities corresponding to smaller number of emerging wave packets. It takes less than ≈ 10 ms of the evolution at the edge of the BZ for the localized wave packets to separate from the surrounding atomic cloud. Similarly to the property of a single gap soliton [7,14], the solitonlike wave packets in the train are immobile in the lattice frame (i.e., have zero group velocity), however, the rest of the atomic cloud is moving with a positive group velocity (to the right). In the laboratory frame the localized wave packets are moving with a finite local velocity to the right, therefore low density “tails” are seen to their left [see Figs. 3(c) and 4(b)].

A single wave packet from the train is shown in Fig. 4(b). For comparison, a density profile of an exact stationary solution of the time-independent NPSE (1) in the form of a

single gap soliton, corresponding to the value of chemical potential $\mu=1.97$ close to the lower edge of the first spectral gap, is presented in Fig. 4(a). Each localized structure in the dynamically generated train extends over $9d \approx 30.6 \mu\text{m}$. The train of matter wave packets of this size can be identified by integrating absorption images as the current experimental detection techniques allow to investigate dynamics of wave packets with $\approx 3 \mu\text{m}$ spatial resolution [8,21]. As in the case with the localized structures generated from an homogeneous Bloch state, the phase structure of the wave packets from the train is similar to that displayed by the gap soliton found numerically as an exact stationary solution of the model equation (1).

V. EFFECT OF ATOM LOSSES

An increase of the density in the dynamically unstable condensate enhances intrinsic inelastic processes, from which the recombination in three-body interatomic collisions is most important. This recombination leads to loss of atoms but does not break the coherence between the particles remaining in the condensate [22]. The three-body loss in the mean-field model can be accounted for by an additional phenomenological term of the form $-i(\hbar/2)K_3|\Phi|^4\Phi$, in the fully 3D Gross-Pitaevskii equation. For ^{87}Rb atoms the three-body recombination rate is measured to be $K_3 = 5.8 \times 10^{-30} \text{ cm}^6 \text{ s}^{-1}$ [23], which in our dimensionless units gives $\kappa_3 = K_3 a_{\perp}^{-6} \omega_{\perp}^{-1} = 5.82 \times 10^{-9}$. In the 1D reduction of the full model, the three-body loss can be accounted for by including the term $-(i/2)\kappa_3|\Psi|^4\Psi$ in the right-hand side of Eq. (1), which at $|\Psi| \ll 1$ is a good approximation of the seemingly more appropriate nonpolynomial term $-i\kappa_3|\Psi|^4(1+\gamma|\Psi|^4)^{-1}\Psi$. The latter has incorrect asymptotics for $|\Psi| \gg 1$ and therefore cannot be used for large condensate densities.

The recombination term in the nonpolynomial model does not exactly correspond to the term usually employed in the 3D GPE (Ref. [22]), and hence values of κ_3 in our model do not exactly match the experimentally measured loss rates. Nevertheless, we have performed simulations for several different values of κ_3 , corresponding to weak to moderate losses. The loss rates of $\kappa_3 \sim 10^{-9}$ do not have any influence

on the dynamics of the condensate cloud neither during the ramp up and acceleration of the lattice nor during the evolution of the BEC at the edge of the BZ. At $\kappa_3 = 10^{-7}$ the losses do not have significant impact during the lattice ramp up, however their effect on the BEC dynamics increases during the acceleration stage and leads to loss of a small fraction of atoms ($\sim 1\%$) from the condensate. The atom loss affects the bulk density moving across the lattice with a nonzero group velocity. However, our simulations show that the enhanced loss of atoms at the moderate three-body loss rates does not suppress the generation of the train of the localized wave packets and does not change the number of the gap soliton-like structures within the train.

In a further study, it would be extremely interesting to investigate effects of the finite temperature and noncondensed fraction on the development of modulational instability and localization of the wave packets in the train.

VI. CONCLUSIONS

We have demonstrated that trains of strongly localized matter-wave wave packets similar to matter-wave gap solitons can be generated as a result of instability of a repulsive condensate adiabatically loaded into an optical lattice and driven to the edge of the first Brillouin zone. This process occurs at moderate numbers of atoms and densities in the initial condensate cloud. Dynamical instability of a nonlinear Bloch state of the BEC thus may provide an alternative soliton-producing mechanism to that employed in the experiment on the formation of a single gap soliton near the band edge [8] where a small atom number was required and a low degree of localization was achieved. Our analysis shows that the time scales of the instability development and characteristic spatial extent of the emerging localized structures are consistent with realistic experimental parameters.

ACKNOWLEDGMENTS

We thank T. J. Alexander, N. P. Robins, and S. Wüster for fruitful discussions, and C. Farrell and M. Kahn for help with the numerics. This research was supported by the Australian Research Council (ARC) and by a grant under the Supercomputer Time Allocation Scheme of the National Facility of the Australian Partnership for Advanced Computing.

-
- [1] L. Fallani, L. De Sarlo, J. E. Lye, M. Modugno, R. Saers, C. Fort, and M. Inuscio, *Phys. Rev. Lett.* **93**, 140406 (2004).
 - [2] M. Cristiani, O. Morsch, N. Malossi, M. Jona-Lasinio, M. Anderlini, E. Courtage, and E. Arimondo, *Opt. Express* **12**, 4 (2004).
 - [3] V. Y. F. Leung, A. G. Truscott, and K. G. H. Baldwin, *Phys. Rev. A* **66**, 061602(R) (2002).
 - [4] K. E. Strecker, G. B. Partridge, A. G. Truscott, and R. G. Hulet, *Nature (London)* **417**, 150 (2002).
 - [5] K. E. Strecker, G. B. Partridge, A. G. Truscott, and R. G. Hulet, *New J. Phys.* **5**, 73 (2003).
 - [6] V. V. Konotop and M. Salerno, *Phys. Rev. A* **65**, 021602(R) (2002).
 - [7] P. J. Louis, E. A. Ostrovskaya, C. M. Savage, and Y. S. Kivshar, *Phys. Rev. A* **67**, 013602 (2003).
 - [8] B. Eiermann, T. Anker, M. Albiez, M. Taglieber, P. Treutlein, K. P. Marzlin, and M. K. Oberthaler, *Phys. Rev. Lett.* **92**, 230401 (2004).
 - [9] H. Pu, L. O. Baksmaty, W. Zhang, N. P. Bigelow, and P. Meystre, *Phys. Rev. A* **67**, 043605 (2003).
 - [10] L. Salasnich, A. Parola, and L. Reatto, *Phys. Rev. A* **65**, 043614(R) (2002).
 - [11] L. Fallani, F. S. Cataliotti, J. Catani, C. Fort, M. Modugno, M. Zawada, and M. Inuscio, *Phys. Rev. Lett.* **91**, 240405 (2003).

- [12] M. Modugno, C. Tozzo, and F. Dalfovo, *Phys. Rev. A* **70**, 043625 (2004); *Phys. Rev. A* **71**, 019904 (2005).
- [13] C. Farrell and U. Leonhardt, *J. Opt. B: Quantum Semiclassical Opt.* **7**, 1 (2005).
- [14] V. Ahufinger, A. Sanpera, P. Pedri, L. Santos, and M. Lewenstein, *Phys. Rev. A* **69**, 053604 (2004).
- [15] J. H. Denschlag, J. E. Simsarian, H. Haffner, C. McKenzie, A. Browaeys, D. Cho, K. Helmerson, S. L. Rolston, and W. D. Phillips, *J. Phys. B* **35**, 3095 (2002).
- [16] P. J. Y. Louis, E. A. Ostrovskaya, and Y. S. Kivshar, *Phys. Rev. A* **71**, 023612 (2005).
- [17] J. Fortadh, H. Ott, G. Schlotterbeck, C. Zimmermann, B. Herzog, and D. Wharam, *Appl. Phys. Lett.* **81**, 1146 (2002).
- [18] L. Pitaevskii and S. Stringari, *Bose-Einstein Condensation* (Clarendon Press, Oxford, 2003), Chap. 17.
- [19] Numerical Recipes: <http://www.library.cornell.edu/nr/>
- [20] E. Peik, M. BenDahan, I. Bouchoule, Y. Castin, and C. Salomon, *Phys. Rev. A* **55**, 2989 (1997).
- [21] Th. Anker, M. Albiez, R. Gati, S. Hunsmann, B. Eiermann, A. Trombettoni, and M. K. Oberthaler, *Phys. Rev. Lett.* **94**, 020403 (2005).
- [22] Yu. Kagan, A. E. Muryshev, and G. V. Shlyapnikov, *Phys. Rev. Lett.* **81**, 933 (1998).
- [23] E. A. Burt, R. W. Ghrist, C. J. Myatt, M. J. Holland, E. A. Cornell, and C. E. Wieman, *Phys. Rev. Lett.* **79**, 337 (1997).